A practical tool for estimating subsurface LNAPL distributions and transmissivity using current and historical fluid levels in groundwater wells: Effects of entrapped and residual LNAPL

R.J. Lenhard[a,c,*], J.L. Rayner[a,c], G.B. Davis[a,b,c]

[a] CSIRO Land and Water, Private Bag No. 5, Wembley, WA 6913, Australia
[b] School of Earth and Environment, University of Western Australia, Nedlands, WA, Australia
[c] Cooperative Research Centre for Contamination Assessment and Remediation of the Environment (CRC CARE), Australia

ABSTRACT

A model is presented to account for elevation-dependent residual and entrapped LNAPL above and below, respectively, the water-saturated zone when predicting subsurface LNAPL specific volume (fluid volume per unit area) and transmissivity from current and historic fluid levels in wells. Physically-based free, residual, and entrapped LNAPL saturation distributions and LNAPL relative permeabilities are integrated over a vertical slice of the subsurface to yield the LNAPL specific volumes and transmissivity. The model accounts for effects of fluctuating water tables. Hypothetical predictions are given for different porous media (loamy sand and clay loam), fluid levels in wells, and historic water-table fluctuations. It is shown the elevation range from the LNAPL-water interface in a well to the upper elevation where the free LNAPL saturation approaches zero is the same for a given LNAPL thickness in a well regardless of porous media type. Further, the LNAPL transmissivity is largely dependent on current fluid levels in wells and not historic levels. Results from the model can aid developing successful LNAPL remediation strategies and improving the design and operation of remedial activities. Results of the model also can aid in accessing the LNAPL recovery technology endpoint, based on the predicted transmissivity.

1. Introduction

Managing remediation activities at sites contaminated with fuel hydrocarbons is still problematic. Fuel hydrocarbons are generally light non-aqueous phase liquids (LNAPL) when in the subsurface. Accurate estimates of subsurface LNAPL distributions are critical for developing successful remedial strategies and improving the design/operation of LNAPL remediation programs (Davis et al., 1993; Johnston et al., 2002; Rayner et al., 2007). Reliable mathematical models are needed (Sookhak Lari et al., 2016a) to predict conditions where the use of LNAPL removal technologies may be effective or when removal technologies are at their remediation end points (e.g., Johnston and Trefry, 2009; Johnston, 2010; Suthersan et al., 2015). Where sufficient LNAPL has entered the subsurface and accumulated on top of water-saturated strata (see e.g., Sookhak Lari et al., 2016b), predicting the potential rate of LNAPL movement into a well after accounting for residual and entrapped LNAPL is valuable for determining if a subsurface LNAPL remediation end point has been reached as well as predicting the fate of the remaining immobile LNAPL.

In this paper, for the first time we present an approach to estimate, under equilibrium conditions, the elevation-dependent distribution of residual and entrapped LNAPL saturations when predicting LNAPL specific volumes (fluid volume per unit area) and transmissivities from fluid levels in wells taking into consideration historic locations of the fluid level elevations in the wells. The model predicts physically-based free, residual, and entrapped saturation distributions and integrates them over the relevant domains to estimate the LNAPL specific volumes and transmissivity from the current fluid levels in the wells and knowledge of their historic fluctuations.

2. Background

An important consideration for remediating sites contaminated with LNAPL is determining the LNAPL volume in the subsurface. Early investigators predicted the LNAPL volume by the LNAPL thickness in wells, the subsurface porosity, and the areal extent of the LNAPL contamination (Hampton and Miller, 1988) assuming a LNAPL saturation of 1, or 1 minus the residual water saturation (van Dam, 1967). It was

understood at the time, however, the actual LNAPL thickness in the subsurface is less than the LNAPL thickness in a well (Schwille, 1967; van Dam, 1967) and using the LNAPL thickness in a well yielded an overestimation of the LNAPL volume in the subsurface. Consequently, the LNAPL thickness in a well was referred to as an apparent thickness. Studies (Zilliox and Muntzer, 1975; de Pastrovich et al., 1979; Hall et al., 1984; Ballestero et al., 1994) related the actual LNAPL thickness in the subsurface to the apparent LNAPL thickness. It was commonly thought the relationship between actual and apparent LNAPL thickness was dependent on grain size of the subsurface formation among other factors (Newell et al., 1995). Further, all LNAPL may not be mobile in the subsurface. Some LNAPL may be entrapped below the water-saturated zone because of water-table elevation fluctuations (hysteresis), which can cause complex relationships between actual and apparent LNAPL thicknesses (Steffy et al., 1995, 1998; Marinelli and Durnford, 1996; Aral and Liao, 2002). Additionally, some LNAPL will be held in small pores and pore wedges in the vadose zone and be relatively immobile (residual). Considerable experimental and field investigations have been undertaken to elucidate NAPL distributions and multiphase relationships (e.g., Lenhard and Parker, 1987; Steffy et al., 1997a, 1997b; Rayner et al., 2000; Johnston and Adamski, 2005). A more fundamental theoretical basis is needed to generalise the approach and for prediction of endpoint transmissivities.

Lenhard and Parker (1990a) and Farr et al. (1990) concluded the actual LNAPL thickness in the subsurface is not a good measure to predict the LNAPL specific volume based on fluid levels in wells. They used well established capillary pressure-saturation fundamental relationships to estimate LNAPL specific volume from fluid levels in wells. In their models, they used nonhysteretic capillary pressure-saturation relations and showed LNAPL and water are variably saturated in the subsurface above the water-saturated zone. A key concept of their efforts was that LNAPL-saturated "pancakes" do not exist. In their models, they did not account for entrapped or residual LNAPL.

From the LNAPL saturations, LNAPL relative permeabilities or transmissivity can be predicted, which can yield useful information for planning remediation activities (Johnston and Trefry, 2009). Parker and Lenhard (1989) developed vertically integrated constitutive relations for predicting LNAPL specific volume and transmissivity in the subsurface from fluid levels in wells. They assumed the LNAPL was mobile, i.e., its relative permeability is greater than zero, whenever the total liquid saturation exceeded the water saturation. Their approach did not account for LNAPL entrapped as ganglia in the water-saturated zone because of water table elevation fluctuations or residual LNAPL in the vadose zone held in pore wedges and other small pore spaces where it is relatively immobile. They further did not account for capillary pressure-saturation hysteresis. Shortly thereafter, Parker et al. (1990, 1994) amended the vertically integrated constitutive relations to consider LNAPL entrapped in the water-saturated zone and residual LNAPL in the unsaturated zone. Their algorithms predicted the total volume of LNAPL entrapped in the water-saturated zone and the total volume of residual LNAPL in the vadose zone for a vertical slice of the subsurface. Because they used vertically integrated constitutive relations, they did not predict elevation-dependent entrapped or residual LNAPL saturations. Later, Waddill and Parker (1997) presented equations for calculating the average entrapped and residual saturations, which were constant values (i.e., invariant) over the water-saturated and unsaturated zones, respectively. Still later, Charbeneau et al. (2000), Charbeneau (2007), and Jeong and Charbeneau (2014) followed the general approach of Waddill and Parker (1997) to calculate average entrapped and residual LNAPL saturations, which also were constant over the water-saturated and unsaturated zones, respectively. Based on calculated average entrapped and residual LNAPL saturations, the free (mobile) LNAPL transmissivity is predicted.

The most accurate technique to predict the behaviour of subsurface LNAPL is to conduct simulations using a multi-dimensional, multiphase flow code with constitutive theory for predicting free, residual, and entrapped LNAPL (e.g., White et al., 2004; Matos de Souza et al., 2016; Sookhak Lari et al., 2016b). Wipfler and van der Zee (2001), Van Geel and Roy (2002), and Lenhard et al. (2004) have developed constitutive capillary pressure-saturation relations for predicting free, entrapped, and residual LNAPL in porous media. Lenhard et al. (2004) also developed saturation-relative permeability relations that account for the entrapped and residual LNAPL, i.e., relative permeability as a function of free LNAPL saturation. In addition to constitutive relations, boundary conditions need to be known (i.e., the rate and volume of LNAPL released, timing and magnitude of potential fluid saturation path changes from precipitation and water table fluctuations, etc.) for multiphase flow codes, which are commonly very uncertain. Furthermore, multiphase flow and transport codes are computationally intensive and typically require sophisticated facilities and training to use the models.

In this paper, we present a method for predicting free, residual, and entrapped LNAPL distributions in the subsurface from limited information relying on current fluid levels in wells and estimations of the maximum fluctuation of the fluid levels. The predictions may be useful to better manage LNAPL remedial activities. Combined with considerations of LNAPL composition (e.g., Sookhak Lari et al., 2016a), the predictions may further be useful for regulation of LNAPL contaminated sites by assisting with informed decisions regarding LNAPL presence and longevity at impacted sites and for risk assessments.

3. Model development

3.1. Fluid pressures

Fluid pressures as a function of elevation in subsurface porous media may be estimated from fluid levels in monitoring wells. For vertical static conditions, the derivatives of total fluid pressures with respect to elevation are zero, i.e.,

$$\frac{\partial P_i}{\partial z} = 0 \tag{1}$$

where P_i is the total pressure of a fluid phase i (i.e., $P_i = p_i + \rho_i g z$) in which p_i is the pressure of fluid phase i, ρ_i is the mass density of fluid phase i, g is the acceleration due to gravity, and z is elevation. The total pressure includes a gravitational (positional) component relative to some datum. The LNAPL and water fluid pressures (p_i), which do not include a gravitational (positional) component, can be expressed as water-equivalent heads, h_i (hereafter referred to only as heads)

$$h_o = \frac{p_o}{g \rho_w} \tag{2}$$

$$h_w = \frac{p_w}{g \rho_w} \tag{3}$$

where the subscripts o and w refer to the LNAPL (or oil) and water, respectively.

For wells screened across LNAPL and water elevations in the subsurface, the LNAPL head for vertical static conditions as a function of elevation (z) above the air-LNAPL interface in a well is

$$h_o = \rho_{ro}(z_{ao} - z) \tag{4}$$

where ρ_{ro} is the LNAPL specific gravity (ratio of LNAPL to water mass density) and z_{ao} is the elevation of the air-LNAPL interface in a well.

For wells screened below any LNAPL in the subsurface, the water head as a function of elevation above the air-water interface in a well is

$$h_w = z_{aw} - z \tag{5}$$

where z_{aw} is the elevation of the air-water interface in a well.

The elevation of the LNAPL-water interface (z_{ow}) in wells screened in the LNAPL and water regions of the subsurface is where the LNAPL-water capillary head [i.e., h_{ow} ($h_{ow} = h_o - h_w$)] is zero and determined by

$$z_{ow} = \frac{z_{aw} - \rho_{ro} z_{ao}}{1 - \rho_{ro}} \qquad (6)$$

Rearranging, the air-water interface (z_{aw}) in a nearby well only screened in the water-saturated region can be determined from

$$z_{aw} = (1 - \rho_{ro})z_{ow} + \rho_{ro} z_{ao} \qquad (7)$$

Accordingly, only two of the three fluid interfaces need to be measured to determine the LNAPL and water heads in the subsurface.

From Eqs. (4), (5), and (7), air-LNAPL and LNAPL-water capillary heads for static conditions as a function of elevation are (Lenhard and Parker, 1990a)

$$h_{ao} = \rho_{ro}(z - z_{ao}) \qquad (8)$$

$$h_{ow} = (1 - \rho_{ro})(z - z_{ow}) \qquad (9)$$

3.2. Fluid saturations

LNAPL and water saturations are functions of the air-LNAPL and LNAPL-water capillary heads (Parker et al., 1987; Lenhard and Parker, 1988)

$$S_o = S_t - S_w = f(h_{ao}, h_{ow}) \qquad (10)$$

$$S_w = f(h_{ow}) \qquad (11)$$

where S_o, S_t, and S_w are the LNAPL, total liquid (LNAPL and water), and water saturations, respectively. The LNAPL, however, can exist as free (mobile), residual (immobile – not occluded by water), and entrapped (immobile - occluded by water as ganglia) LNAPL. The free LNAPL is important for assessing potential movement of LNAPL during subsurface LNAPL extraction from wells and for assessing risks of subsurface migration.

To calculate actual free, residual, and entrapped LNAPL saturations in water-wet porous media as a function of the air-LNAPL and LNAPL-water capillary heads, apparent saturations are used as defined by Lenhard et al. (2004)

$$\bar{\bar{S}}_t = \frac{S_w + S_o + S_{ae} - S_{wr}}{1 - S_{wr}} \qquad (12)$$

$$\bar{\bar{S}}_w = \frac{S_w + S_{oe} + S_{aew} - S_{wr}}{1 - S_{wr}} \qquad (13)$$

where $S_o = S_{of} + S_{oe} + S_{or}$ and $S_{ae} = S_{aew} + S_{aeo}$, in which
$\bar{\bar{S}}_t$ = apparent total-liquid saturation (LNAPL and water).
$\bar{\bar{S}}_w$ = apparent water saturation.
S_{of} = actual free (mobile) LNAPL saturation.
S_{oe} = actual entrapped LNAPL saturation.
S_{or} = actual residual LNAPL saturation.
S_{ae} = actual total entrapped air saturation in water and LNAPL ($S_{ae} = S_{aew} + S_{aeo}$).
S_{aew} = actual entrapped air saturation in water.
S_{aeo} = actual entrapped air saturation in LNAPL.
S_{wr} = actual residual water saturation.

Apparent saturations include entrapped non-wetting saturations within the corresponding wetting fluids. For LNAPL contamination, the apparent water saturation is a scaled saturation including water, entrapped LNAPL, and entrapped air. It indexes the largest pores in which water occurs to obtain better estimates of the water relative permeability. The apparent total liquid saturation is a scaled saturation including water, LNAPL, and entrapped air. It indexes the largest pores in which LNAPL occurs to obtain better estimates of the LNAPL relative permeability.

Subtracting the apparent water saturation from the apparent total-liquid saturation yields

$$\bar{\bar{S}}_t - \bar{\bar{S}}_w = \frac{S_w + S_o + S_{ae} - S_{wr} - S_w - S_{oe} - S_{aew} + S_{wr}}{1 - S_{wr}} \qquad (14a)$$

$$= \frac{S_{of} + S_{or} + S_{aeo}}{1 - S_{wr}} \qquad (14b)$$

Neglecting S_{aeo} for simplicity, because it realistically only represents a small volume and unlikely to be a significant factor in subsurface LNAPL extraction from wells, gives an expression for estimating the actual free LNAPL saturation

$$S_{of} = (1 - S_{wr})(\bar{\bar{S}}_t - \bar{\bar{S}}_w) - S_{or} \qquad (15)$$

Following Lenhard et al. (2004), the actual residual LNAPL saturation depends on three factors: a calibration term, which is the maximum actual residual LNAPL saturation likely to occur in a porous medium; the volume of pore space occupied by the LNAPL; and an index to the size of the pores containing the LNAPL. They proposed an equation of the form

$$S_{or} = (1 - S_{wr})AB^\lambda C^\eta \qquad (16)$$

where A is the calibration term, B represents the volume of pore space occupied by LNAPL, C is an index to the size of the pores containing the LNAPL, and λ and η are power terms applied to the factors. Their final equation was

$$S_{or} = S_{or}^{max}(\bar{\bar{S}}_t^{max} - \bar{\bar{S}}_w)^{0.5} (1 - \bar{\bar{S}}_w)^{1.5} \qquad (17)$$

where S_{or}^{max} is the maximum actual residual LNAPL saturation of a porous medium and $\bar{\bar{S}}_t^{max}$ is the historic maximum apparent total-liquid saturation. S_{or}^{max} is the term A in Eq. (16), $\bar{\bar{S}}_t^{max} - \bar{\bar{S}}_w$ is the term B, and $1 - \bar{\bar{S}}_w$ is the term C. To calculate S_{of} using Eq. (15), S_{or} is first calculated using Eq. (17) and then substituted in Eq. (15) where $\bar{\bar{S}}_t$, $\bar{\bar{S}}_w$, and $\bar{\bar{S}}_t^{max}$ are functions of the saturation path history (capillary heads).

The actual entrapped LNAPL, S_{oe}, for a water-wet porous media is estimated by scaling the actual entrapped LNAPL saturation resulting from water imbibition into an initially LNAPL-saturated porous medium until it is apparently water saturated (i.e., possessing only entrapped LNAPL and continuous water), which is the maximum actual entrapped LNAPL saturation of the main imbibition branch (i.e., S_{oe}^{max}). The scaling yields $S_{oe} = 0$ when $\bar{\bar{S}}_w = \bar{\bar{S}}_w^{min}$ and a maximum value less than S_{oe}^{max} when $\bar{\bar{S}}_w = 1$ and $\bar{\bar{S}}_w^{min} > 0$. When $\bar{\bar{S}}_w = 1$ and $\bar{\bar{S}}_w^{min} = 0$, then $S_{oe} = S_{oe}^{max}$.

Using this approach for elevations higher than z_{ow}, the actual entrapped LNAPL saturation is

$$S_{oe} = S_{oe}^{max} (\bar{\bar{S}}_w - \bar{\bar{S}}_w^{min}) \qquad (18)$$

where S_{oe}^{max} is the maximum actual entrapped LNAPL saturation and $\bar{\bar{S}}_w^{min}$ is the historic minimum apparent water saturation and represents the smallest pores in which LNAPL was present.

For elevations lower than or equal to z_{ow}, i.e., $\bar{\bar{S}}_w = 1$, the actual entrapped LNAPL saturation is

$$S_{oe} = S_{oe}^{max} (1 - \bar{\bar{S}}_w^{min}) \qquad (19)$$

For elevations lower than the LNAPL-water fluid level in the well corresponding to the establishment of $\bar{\bar{S}}_w^{min}$ (i.e., z_{ow}^{min}), then $S_{oe} = 0$ because $\bar{\bar{S}}_w$ will equal $\bar{\bar{S}}_w^{min}$. Note at z_{ow}, Eqs. (18) and (19) yield the same value. The scaling procedure will likely eliminate the issue Kaluarachchi and Parker (1992) found using the approach of Parker and Lenhard (1987) for estimating entrapped LNAPL.

$\bar{\bar{S}}_t$, $\bar{\bar{S}}_w$, $\bar{\bar{S}}_t^{max}$, and $\bar{\bar{S}}_w^{min}$ as functions of the air-LNAPL and LNAPL-water capillary heads are obtained from appropriate saturation-pressure functions (e.g., Brooks and Corey, 1966; van Genuchten, 1980). Either nonhysteretic (similar to Parker et al., 1987) or hysteretic (similar to Parker and Lenhard, 1987; Lenhard et al., 2004) constitutive relations can be employed. Historic and/or current fluid interfaces (z_{ao} and z_{ow}) determine the capillary heads as a function of elevation.

3.3. Fluid volumes

Volumes of LNAPL at vertical static conditions in a vertical slice of the subsurface within a representative distance from a well are estimated by integrating S_{of}, S_{or}, and S_{oe} over relevant depths of the subsurface.

S_{of} is integrated over the relevant elevations to obtain the actual free LNAPL volume (V_{of}) per unit cross-sectional area in the horizontal plane

$$V_{of} = \int_{z_{ow}}^{z_u} \phi S_{of} \, dz \tag{20}$$

where ϕ is the porosity per unit cross-sectional area in the horizontal plane, and z_u and z_{ow} present the elevation range at which LNAPL is present. z_u is either the ground surface if LNAPL was released at the surface and migrated downwards to the aquifer or the upper elevation where continuous $\overline{\overline{S}}_t$ equals $\overline{\overline{S}}_w$ based on current fluid levels in a well. z_{ow} is the lower elevation where free LNAPL is present because at lower elevations the subsurface will be apparently water saturated (i.e., water saturated with possible entrapped LNAPL); it is the elevation where $h_{ow} = 0$ [see Eq. (9)]. To calculate V_{of}, Eq. (15) is used in Eq. (20) to yield

$$V_{of} = \phi(1 - S_{wr}) \left[\int_{z_{ow}}^{z_u} \overline{\overline{S}}_t \, dz - \int_{z_{ow}}^{z_u} \overline{\overline{S}}_w \, dz \right] - V_{or} \tag{21}$$

where V_{or} is the actual residual LNAPL volume in a vertical slice of the subsurface per unit cross-sectional area in the horizontal plane.

To determine z_u following Lenhard and Parker (1990b), continuous $\overline{\overline{S}}_t$ equals $\overline{\overline{S}}_w$ when

$$\beta_{ao}\rho_{ro}(z - z_{ao}) = \beta_{ow}(1 - \rho_{ro})(z - z_{ow}) \tag{22a}$$

yielding

$$z = \frac{\beta_{ao}\rho_{ro}z_{ao} - \beta_{ow}(1 - \rho_{ro})z_{ow}}{\beta_{ao}\rho_{ro} - \beta_{ow}(1 - \rho_{ro})} \tag{22b}$$

where β_{ao} and β_{ow} are ratios of interfacial tensions accordingly

$$\beta_{ao} = \frac{\sigma_{ao} + \sigma_{ow}}{\sigma_{ao}} \tag{23}$$

$$\beta_{ow} = \frac{\sigma_{ao} + \sigma_{ow}}{\sigma_{ow}} \tag{24}$$

where σ_{ao} and σ_{ow} are air-LNAPL and LNAPL-water interfacial tensions. Therefore,

$$z_u = \begin{cases} \text{elevation of ground surface, if applicable} \\ \text{or} \\ \dfrac{\beta_{ao}\rho_{ro}z_{ao} - \beta_{ow}(1 - \rho_{ro})z_{ow}}{\beta_{ao}\rho_{ro} - \beta_{ow}(1 - \rho_{ro})} \end{cases} \tag{25}$$

Note that the elevation where continuous $\overline{\overline{S}}_t$ equals $\overline{\overline{S}}_w$ is not dependent on any porous medium properties; it is only a function of fluid properties, z_{ao}, and z_{ow}. Therefore, the upper elevation at which free LNAPL exists in the subsurface is only a function of fluid properties and prevailing capillary pressures (i.e., fluid levels in a nearby well); it is not a function of porous media properties.

S_{or} is integrated over relevant elevations to obtain the actual residual LNAPL volume (V_{or}) per unit cross-sectional area in the horizontal plane

$$V_{or} = \int_{z_{ow}}^{z_u} \phi S_{or} \, dz + \int_{z_u}^{z_u^{max}} \phi S_{or} \, dz \tag{26}$$

where z_u^{max} is either the elevation where there was no free LNAPL when the fluid levels in the wells were at their historical highest levels, i.e., z_{ao}^{max} and z_{ow}^{max}, or the ground surface. Therefore, z_u^{max} is determined using Eq. (25) with substituting z_{ao}^{max} for z_{ao} and z_{ow}^{max} for

z_{ow}. Provided no additional LNAPL volume was added to the system, z_{ow}^{max} should equal $z_{ow} + (z_{ao}^{max} - z_{ao})$; the same increase in elevation as with the z_{ao} levels. V_{or} has two components: one is S_{or} in the elevation range from the water-saturated zone to where no continuous LNAPL exists based on the current z_{ao} and z_{ow} or the ground surface, and the second is S_{or} in the elevation range from where no continuous LNAPL exists based on current the current z_{ao} and z_{ow}, if not the ground surface, to either where no continuous LNAPL existed when z_{ao}^{max} and z_{ow}^{max} occurred or the ground surface. Note that if z_u equals the ground surface elevation, then z_u^{max} also will equal the ground surface, and the second term in Eq. (26) drops out.

Using Eq. (17), V_{or} is determined accordingly

$$V_{or} = \phi S_{or}^{max} \left\{ \int_{z_{ow}}^{z_u} (\overline{\overline{S}}_t^{max} - \overline{\overline{S}}_w)^{0.5} \, (1 - \overline{\overline{S}}_w)^{1.5} \, dz \right. $$
$$\left. + \int_{z_u}^{z_u^{max}} (\overline{\overline{S}}_t^{max} - \overline{\overline{S}}_w)^{0.5} \, (1 - \overline{\overline{S}}_w)^{1.5} \, dz \right\} \tag{27}$$

where $\overline{\overline{S}}_t^{max}$ is determined from the air-LNAPL capillary head corresponding with z_{ao}^{max}. $\overline{\overline{S}}_w$ is determined from the LNAPL-water capillary heads corresponding to the elevations between z_{ow} and z_u or z_{ao}^{max}.

S_{oe} is integrated over relevant elevations to obtain the actual entrapped LNAPL volume (V_{oe}) per unit cross-sectional area in the horizontal plane

$$V_{oe} = \int_{z_{ow}^{min}}^{z_u} \phi S_{oe} \, dz \tag{28}$$

where z_{ow}^{min} is the historical lowest LNAPL-water fluid level in the well.

Using Eqs. (18) and (19), V_{oe} is determined accordingly

$$V_{oe} = \phi \int_{z_{ow}^{min}}^{z_{ow}} S_{oe}^{max}(1 - \overline{\overline{S}}_w^{min}) \, dz + \phi \int_{z_{ow}}^{z_u} S_{oe}^{max}(\overline{\overline{S}}_w - \overline{\overline{S}}_w^{min}) \, dz \tag{29}$$

where $\overline{\overline{S}}_w^{min}$ is determined from the LNAPL-water capillary head corresponding to z_{ow}^{min}. $\overline{\overline{S}}_w$ is determined from the LNAPL-water capillary heads corresponding to the elevations between z_{ow} and z_u.

For cases where the LNAPL-water interface in a well was never below the current elevation of the LNAPL-water interface, then V_{oe} is zero. For such a condition, the left integral in Eq. (29) is zero because z_{ow}^{min} would equal z_{ow}. The right integral also is zero because $\overline{\overline{S}}_w$ would equal $\overline{\overline{S}}_w^{min}$ for all elevations between z_{ow} and z_u.

V_{of}, V_{or}, and V_{oe} can be estimated from the current and historical fluid levels in wells. The total LNAPL volume in a vertical slice of the subsurface is obtained by summing V_{of}, V_{or}, and V_{oe}.

3.4. Fluid transmissivity

Additional important information for managing LNAPL extraction from wells or assessing future contamination risks is the potential movement and recoverability of the free (mobile) LNAPL. Such a measure is the LNAPL transmissivity, which includes potential contributions of LNAPL flow along a vertical slice of the subsurface. The magnitude of the contributions is a function of elevation because S_{of} varies with elevation as does h_{ao} and h_{ow}. The largest potential contributions come from regions of the subsurface where the LNAPL is in the largest pore sizes. This occurs when S_t approaches 1 when free LNAPL is present. Smaller potential contributions result when S_t is < 1, because the LNAPL is contained in smaller and smaller pores as S_t becomes lower as h_{ao} increases. When S_t approaches S_w, the potential contributions are negligible. To account for the varying potential contributions with elevation in a vertical slice of the subsurface, the LNAPL hydraulic conductivities (K_o) as a function of S_t and S_w are summed over the elevations where LNAPL is present to obtain the LNAPL transmissivity (T_o)

$$T_o = \int_{z_{ow}}^{z_u} K_o \, dz \tag{30}$$

The LNAPL hydraulic conductivities (K_o) are determined from multiplying the LNAPL relative permeability (k_{ro}) by the water-saturated hydraulic conductivity (K_{sw})

$$K_o = \frac{\rho_{ro} K_{sw}}{\eta_{ro}} k_{ro} \tag{31}$$

where η_{ro} is the ratio of LNAPL to water viscosity. Therefore, T_o is determined from the elevation-dependent LNAPL relative permeabilities

$$T_o = \frac{\rho_{ro} K_{sw}}{\eta_{ro}} \int_{z_{ow}}^{z_u} k_{ro} \, dz \tag{32}$$

Following Lenhard et al. (2004) and after neglecting effects of S_{aeo}, k_{ro} is estimated from

$$k_{ro} = \overline{\overline{S_{of}}}^{\,0.5} \left\{ \frac{\int_{\overline{\overline{S}}_w + \overline{S}_{or}}^{\overline{\overline{S}}_t} \frac{d\overline{S}}{h(\overline{S})}}{\int_0^1 \frac{d\overline{S}}{h(\overline{S})}} \right\}^2 \tag{33}$$

where $\overline{S}_{of}$ and $\overline{S}_{or}$ are effective free and residual LNAPL saturations, respectively, defined as

$$\overline{S}_{of} = \frac{S_{of}}{1 - S_{wr}} \tag{34}$$

$$\overline{S}_{or} = \frac{S_{or}}{1 - S_{wr}} \tag{35}$$

and $1/h(\overline{S})$ is a surrogate for the pore-size distribution of a porous medium, which will depend on the capillary head-saturation function used (e.g., Brooks and Corey, 1966; van Genuchten, 1980). Note k_{ro} depends on the current and historical z_{ow} and z_{ao} because the values are used to calculate $\overline{\overline{S}}_t$, $\overline{\overline{S}}_w$, $\overline{S}_{of}$ and $\overline{S}_{or}$.

After integrating the terms in Eq. (33) following Lenhard et al. (2004), k_{ro} is calculated as

$$k_{ro} = \overline{S}_{of}^{\,0.5} \{ [1 - (\overline{\overline{S}}_w + \overline{S}_{or})^{1/m}]^m - (1 - \overline{\overline{S}}_t^{\,1/m})^m \}^2 \tag{36}$$

where m is a van Genuchten (1980) parameter. T_o [Eq. (30)] will need to be numerically estimated using Eq. (36).

Estimating V_{of}, V_{or}, V_{oe}, and T_o are important for managing subsurface LNAPL recovery from wells because the information can be used to assess potential future risks and conditions where physical extraction of LNAPL is warranted practically and economically.

4. Model applications & discussions

To show results from applying the model, predicted subsurface free, residual, and entrapped LNAPL distributions are calculated for two general saturation path scenarios. Predicted LNAPL transmissivities are calculated from the LNAPL distributions and compared to calculations not accounting for residual and entrapped LNAPL. Parameters used to predict the LNAPL distributions and transmissivities are shown in Table 1. There are two sets of parameters: one set to describe hydraulic properties of hypothetical porous media and one set to describe hypothetical fluid properties. We employ the van Genuchten (1980) function to describe relations between apparent saturations (i.e., $\overline{\overline{S}}_t$, $\overline{\overline{S}}_w$, $\overline{\overline{S}}_t^{\,max}$, and $\overline{\overline{S}}_w^{\,min}$) and capillary heads from fluid levels in wells. Furthermore, we use the van Genuchten (1980) function as described in Parker et al. (1987) for air, LNAPL, water systems, i.e., a monotonic function. We consider two porous media: one representing a sandy porous medium (loamy sand) and one representing a finer textured porous medium (clay loam). The hydraulic properties and van Genuchten parameters for a loamy sand and a clay loam are from Carsel

Table 1
Assumed properties and parameters.

Hypothetical hydraulic properties and parameters		
	Loamy sand	Clay loam
α (cm^{-1})	0.124	0.019
n	2.28	1.31
S_{wr} (cm^3 cm^{-3})	0.139	0.232
Φ (cm^3 cm^{-3})	0.41	0.41
K_{sw} (cm day^{-1})	350	6.24
S_{or}^{max} (cm^3 cm^{-3})	0.15	0.20
S_{oe}^{max} (cm^3 cm^{-3})	0.15	0.20
Hypothetical fluid properties		
σ_{ow} (mN m^{-1})		29
σ_{ao} (mN m^{-1})		36
ρ_{ro}		0.73
η_{ro}		0.8

and Parrish (1988). The saturated water content is assumed to equal the porosity. The maximum actual residual and entrapped saturations for the loamy sand and clay loam are assumed to be 0.15 and 0.20, respectively, which are consistent with values reported by Mercer and Cohen (1990). Hypothetical fluid properties are representative of gasoline (petrol) and the LNAPL-water and air-LNAPL interfacial tensions yield β_{ao} and β_{ow} scaling factors used by Lenhard et al. (2004) from Eqs. (23) and (24), respectively. The specific gravity (ρ_{ro}) is consistent with Mercer and Cohen (1990) and the ratio of LNAPL to water viscosity (η_{ro}) is consistent with Parker and Lenhard (1989).

Saturation path history needs to be considered when using Eqs. (20), (26), and (29) to calculate LNAPL distributions and Eq. (30) to calculate LNAPL transmissivities. To show model predictions, we use two saturation path scenarios. They do not reflect actual LNAPL contamination events; they are designed to show elements of the model. *Scenario A* is when (i) z_{ao}^{max} equals the current z_{ao} (i.e., the air-LNAPL level in a well was never at a higher elevation), and (ii) when z_{ow}^{min} equals the current z_{ow} (i.e., the LNAPL-water level in a well was never at lower elevation). For this scenario, there is no entrapped LNAPL and only residual LNAPL will occur between the upper elevation of complete water saturation (i.e., z_{ow}) and the elevation where $\overline{\overline{S}}_t$ equals $\overline{\overline{S}}_w$, i.e., where no continuous LNAPL is present. The residual LNAPL will be generally in pore wedges and films, which is considered to be immobile relative to the LNAPL in the larger pores spaces.

The other scenario, which we will call *Scenario B*, is when z_{ao}^{max} was at a higher elevation prior to the current z_{ao} and z_{ow}^{min} was at a lower elevation prior to the current z_{ow}. When z_{ao}^{max} is at a higher elevation than the current z_{ao}, residual LNAPL will develop as in *Scenario A*. As the air-LNAPL level in a well declines from z_{ao}^{max} to the current z_{ao}, the amount of residual LNAPL may change at an elevation as $\overline{\overline{S}}_t^{\,max}$ and $\overline{\overline{S}}_w$ changes [see Eq. (17)], but it will never become less after the maximum amount is established, because that amount is immobile. The result will be a minor amount of residual LNAPL at elevations close to where $\overline{\overline{S}}_t$ equals $\overline{\overline{S}}_w$ when z_{ao}^{max} was established (i.e., z_u^{max}) with greater amounts of residual LNAPL at lower elevations until a maximum specific to the saturation path is established. Once the maximum residual LNAPL is established at an elevation, all elevations below that level will be at that maximum until lower elevations are reached where conditions necessary to form the maximum residual LNAPL will never be created. For these elevations, the residual LNAPL formed will be less than the maximum and approach zero as the elevation approaches the LNAPL-water level in the well. z_{ao}^{max} may be known from well data or estimated based on historic water-table fluctuations.

Under *Scenario B*, entrapped LNAPL will exist between elevations z_{ow}^{min} and z_{ow} because z_{ow}^{min} was at a lower elevation than the current z_{ow}. Free LNAPL at these elevations would move upwards or become

occluded by water (i.e., entrapped) as the LNAPL-water level in the well rises from z_{ow}^{min} to the current z_{ow}. Residual LNAPL between these elevations may become entrapped. For elevations below z_{ow}, $\bar{\bar{S}}_w$ will equal 1 and only water and entrapped LNAPL will exist. For elevations above z_{ow}, entrapped LNAPL also may exist because the current $\bar{\bar{S}}_w$ at an elevation will be higher than the $\bar{\bar{S}}_w$ when z_{ow}^{min} was established (i.e., $\bar{\bar{S}}_w^{min}$). A minor amount of entrapped LNAPL may exist until an elevation where $\bar{\bar{S}}_t$ equals $\bar{\bar{S}}_w$.

For *Scenario B*, we feel whether z_{ao}^{max} or z_{ow}^{min} is established first will not significantly affect the predicted free, residual, and entrapped LNAPL distributions because z_{ao}^{max} is the major parameter for establishing the residual LNAPL distribution and z_{ow}^{min} is the major parameter for establishing the entrapped LNAPL distribution. This is an assumption. The current z_{ao} and z_{ow} mainly establishes the free LNAPL distribution. Variants of *Scenario B* are when z_{ao} is raised or z_{ow} are lowered independently. The following sections illustrate the free, residual, and entrapped LNAPL saturation distributions likely to develop from *Scenarios A and B* and the resulting estimated LNAPL transmissivities and volumes.

4.1. Scenario A

Fig. 1 shows the predicted free (mobile), residual, and entrapped LNAPL saturations resulting from a LNAPL thickness of 50 cm inside a nearby well for the loamy sand porous medium. Also shown are the LNAPL saturations when there is no accounting for residual or entrapped LNAPL, i.e., all of the LNAPL is considered to be free. Fig. 3a shows the actual total liquid and water saturations. The elevations of z_{ao} and z_{ow} are assumed to be 150 cm and 100 cm, respectively. We calculate the predictions assuming z_{ao}^{max} equals the current z_{ao} (150 cm) and z_{ow}^{min} equals the current z_{ow} (100 cm).

No entrapped LNAPL is predicted and residual LNAPL will only occur from z_{ow} to the elevation where $\bar{\bar{S}}_t$ equals $\bar{\bar{S}}_w$ (i.e., z_u), which is at approximately 192 cm for the assumed fluid properties and well fluid levels. When summing the free, residual, and entrapped LNAPL saturations over the domain, the total LNAPL saturations closely matched the saturations distribution when not considering residual and entrapped LNAPL, i.e., using the model of Lenhard and Parker (1990a). We label saturation distributions when not considering residual and entrapped LNAPL as short broken black lines in the figures, which is the model of Lenhard and Parker (1990a). Even without any fluid level fluctuations in the well, less free LNAPL volume is estimated when including residual LNAPL. The predicted free LNAPL volume was 85.2% of the total LNAPL volume. The largest residual LNAPL saturation for
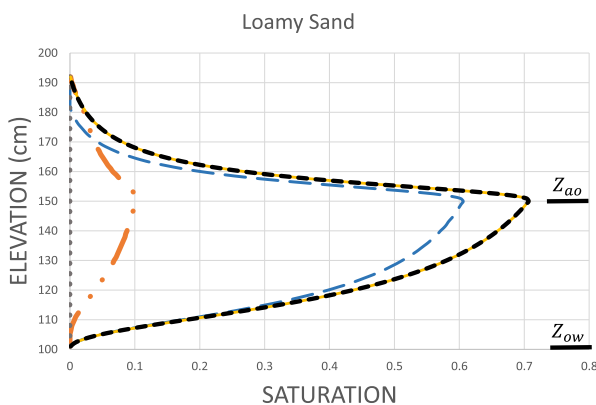
Fig. 1. Predicted free (longer broken blue lines), residual (broken orange lines separated by two dots), entrapped (dotted grey line), and total (solid yellow line) LNAPL saturations as a function of elevation for the loamy sand where z_{ao} and z_{ao}^{max} = 150 cm and z_{ow} and z_{ow}^{min} = 100 cm elevations with S_{or}^{max} and S_{oe}^{max} = 0.15. The shorter broken black lines are estimates using the model of Lenhard and Parker (1990a). (For interpretation of the references to colour in this figure legend, the reader is referred to the web version of this article.)
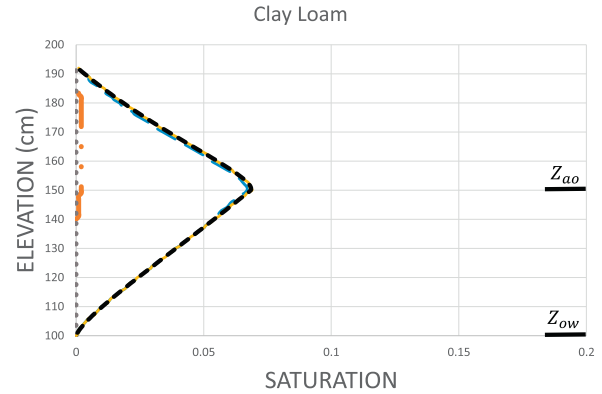
Fig. 2. Predicted free (longer broken blue lines), residual (broken orange lines separated by two dots), entrapped (dotted grey line), and total (solid yellow line) LNAPL saturations as a function of elevation for the clay loam where z_{ao} and z_{ao}^{max} = 150 cm and z_{ow} and z_{ow}^{min} = 100 cm elevations with S_{or}^{max} and S_{oe}^{max} = 0.2. The shorter broken black lines are estimates using the model of Lenhard and Parker (1990a). (For interpretation of the references to colour in this figure legend, the reader is referred to the web version of this article.)

the scenario was 0.1 at z_{ao}, because the difference between $\bar{\bar{S}}_t^{max}$ and $\bar{\bar{S}}_w$ will be the greatest at z_{ao} where $\bar{\bar{S}}_t^{max}$ will equal 1 [see Eq. (17)]. The amount of residual LNAPL decreases with increasing elevation and will approach zero at z_u. The net effect will be to reduce the predicted LNAPL transmissivity relative to when no residual LNAPL is estimated. The predicted LNAPL transmissivity for the scenario when accounting for residual LNAPL is 4294 cm^2 day^{-1} [4.62 ft^2 day^{-1}]. The predicted LNAPL transmissivity when not accounting for residual LNAPL is 6506 cm^2 day^{-1} [7.0 ft^2 day^{-1}] – a 51.5% increase. Consequently, lower predicted LNAPL transmissivities will result when accounting for residual LNAPL, which is important to consider when managing LNAPL extraction from wells.

Fig. 2 shows the predicted free, residual, and entrapped LNAPL saturations for the clay loam porous medium using the same conditions as for the loamy sand in Fig. 1. Fig. 3b shows the actual total liquid and water saturations. The striking difference is the low total LNAPL volume predicted for the same LNAPL thickness in a well for the clay loam. The total LNAPL volume predicted in the loamy sand for a 50 cm LNAPL well thickness is 12.30 cm^3 cm^{-2}, whereas for the clay loam it is 1.27 cm^3 cm^{-2}. This highlights the large potential errors involved in estimating LNAPL volumes from in-well thicknesses without accounting for porous media and fluid properties.

Approximately 97% of the total volume is predicted to be free LNAPL largely because of the small amount of LNAPL predicted to be in the clay loam. The difference in LNAPL volume predicted to be in the loamy sand versus the clay loam is attributed to the difference in pore-size distributions. The loamy sand has larger-sized pores than does the clay loam, despite the same porosity. As a result, the loamy sand is able to contain more LNAPL than the clay loam under the prevailing capillary heads. A key element that may not be commonly understood is the LNAPL thickness in subsurface media [i.e., the region of the subsurface from where the LNAPL-water capillary head is zero (i.e., z_{ow}) to where the total liquid saturation equals the water saturation (i.e., z_u)] is the same for all porous media with the same fluid properties and fluid levels in a well. As discussed in the Model Development section, z_u is only a function of fluid properties and the LNAPL thickness in a well. There are no factors involving porous media properties, such as a pore-size distribution. Hence, the same LNAPL thickness from z_{ow} to where $\bar{\bar{S}}_t$ equals $\bar{\bar{S}}_w$ is predicted to be in the loamy sand as in the clay loam, but the loamy sand has larger pores to hold the LNAPL and the water saturation above z_{ow} will be less in the loamy sand than in the clay loam, i.e., a larger capacity to hold LNAPL. If a distinct capillary fringe occurs (i.e., a completely water-saturated zone above z_{ow}) and has a different thickness for the loamy sand and clay loam, then the elevation range
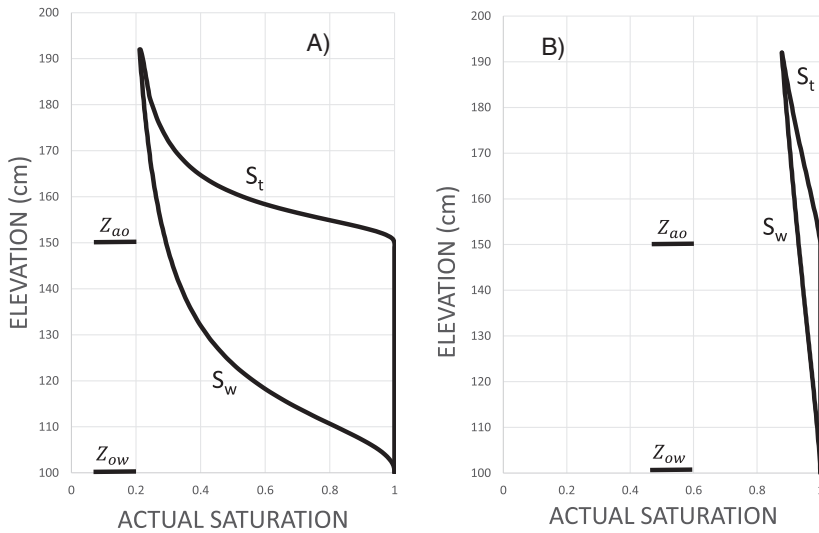
Fig. 3. Actual total liquid and water saturation distributions in the loamy sand (A) and clay loam (B) for *Scenario A*.

over which LNAPL will exist in the loamy sand and clay loam will be different, because of the difference in the thickness of the capillary fringe. However, given there may be larger void spaces because of heterogeneities (i.e., secondary pore/soil structure, old root channels, etc.), some LNAPL may extend down to z_{ow} even if a capillary fringe is apparent. Fig. 3 shows the actual total liquid and water saturation distributions for the loamy sand and clay loam for the assumed conditions.

Although the residual LNAPL in Fig. 2 is small, it still affects the predicted LNAPL transmissivity. When accounting for the residual LNAPL, the predicted LNAPL transmissivity for the clay loam is 2.35 cm^2 day^{-1} [2.53 × 10^{-3} ft^2 day^{-1}]. When not accounting for residual LNAPL, the predicted LNAPL transmissivity is 2.50 cm^2 day^{-1} [2.69 × 10^{-3} ft^2 day^{-1}] - a 6.4% increase.

4.2. Scenario B

In *Scenario B*, z_{ao}^{max} may be higher than the current z_{ao} and z_{ow}^{min} may be lower than the current z_{ow}. This scenario reflects fluctuating fluid levels in the subsurface, and in this instance the maximum upper and lower extent that the respective interfaces achieved in a monitoring well. Under this scenario, we predict free, residual, and entrapped LNAPL distributions for several LNAPL thicknesses in a well and for a slight increase in S_{or}^{max} and S_{oe}^{max}.

Figs. 4–6 show the predicted free, residual, and entrapped LNAPL saturations for the loamy sand when z_{ao}^{max} at one time was 50 cm above the current z_{ao} and z_{ow}^{min} at one time was 50 cm below the current z_{ow} for several LNAPL well thicknesses. Figs. 4, 5, and 6 show the LNAPL distributions when the LNAPL well thickness was 25, 50, and 100 cm, respectively. The elevations of the fluid interfaces in the well are marked on the right side of the figures. The scale of the figures is the same so relative differences in LNAPL saturations for the different well thicknesses can be seen. In Fig. 4, the current z_{ao} and z_{ow} is at 150 and 125 cm, respectively. Because z_{ow}^{min} was lower at one time, water is on an imbibition saturation path, which results in entrapped LNAPL. Between z_{ow}^{min} and z_{ow} only entrapped LNAPL is present as shown by the dotted grey line. The total LNAPL saturation (solid yellow line) will equal the entrapped LNAPL saturation for these elevations. Free, residual, and entrapped LNAPL is present between z_{ow} and z_u, which is approximately 171 cm for these z_{ao} and z_{ow}. Above 171 cm to where $\overline{\overline{S}}_t$ equaled $\overline{\overline{S}}_w$ when z_{ao}^{max} was established (i.e., z_u^{max}), only residual and entrapped is present. Entrapped LNAPL is present because the current z_{ow} indicates water is on an imbibition path at these elevations which can entrap LNAPL (i.e., $z_{ow} > z_{ow}^{min}$). Residual LNAPL is present because the current z_{ao} indicates LNAPL was present forming residual
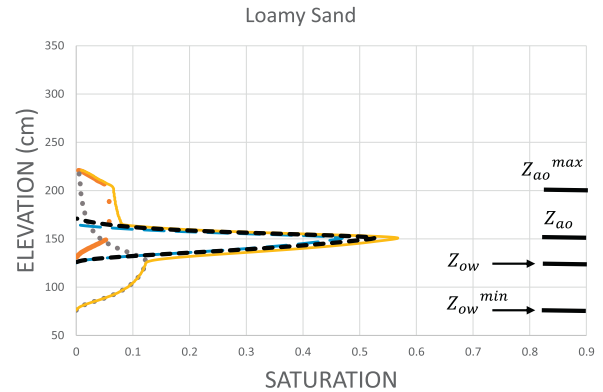
Fig. 4. Predicted free (longer broken blue lines), residual (broken orange lines separated by two dots), entrapped (dotted grey line), and total (solid yellow line) LNAPL saturations as a function of elevation for the loamy sand where z_{ao} = 150 cm, z_{ow} = 125 cm, z_{ao}^{max} = 200 cm, and z_{ow}^{min} = 75 cm elevations with S_{or}^{max} and S_{oe}^{max} = 0.15. The shorter broken black lines are estimates using the model of Lenhard and Parker (1990a). (For interpretation of the references to colour in this figure legend, the reader is referred to the web version of this article.)
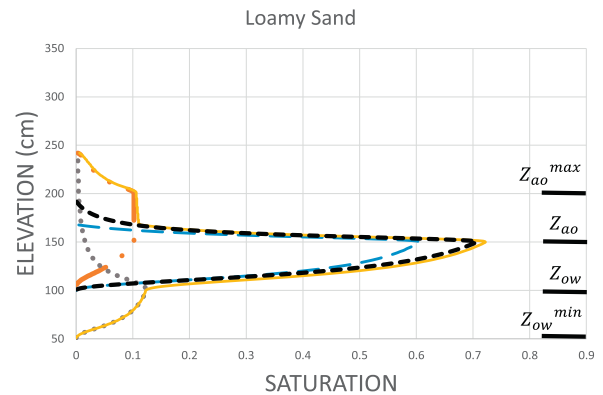
Fig. 5. Predicted free (longer broken blue lines), residual (broken orange lines separated by two dots), entrapped (dotted grey line), and total (solid yellow line) LNAPL saturations as a function of elevation for the loamy sand where z_{ao} = 150 cm, z_{ow} = 100 cm, z_{ao}^{max} = 200 cm, and z_{ow}^{min} = 50 cm elevations with S_{or}^{max} and S_{oe}^{max} = 0.15. The shorter broken black lines are estimates using the model of Lenhard and Parker (1990a). (For interpretation of the references to colour in this figure legend, the reader is referred to the web version of this article.)
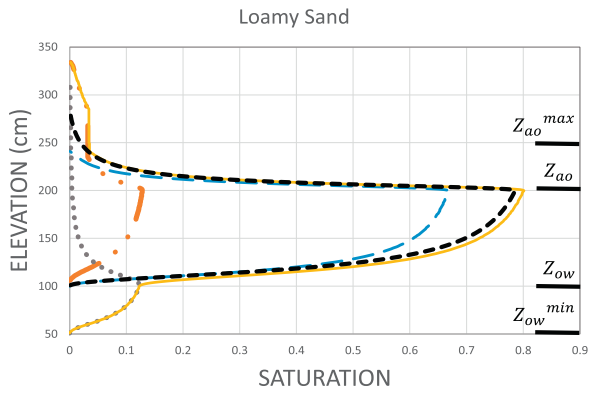
Fig. 6. Predicted free (longer broken blue lines), residual (broken orange lines separated by two dots), entrapped (dotted grey line), and total (solid yellow line) LNAPL saturations as a function of elevation for the loamy sand where $z_{ao} = 200$ cm, $z_{ow} = 100$ cm, $z_{ao}{}^{max} = 250$ cm, and $z_{ow}{}^{min} = 50$ cm elevations with $S_{or}{}^{max}$ and $S_{oe}{}^{max} = 0.15$. The shorter broken black lines are estimates using the model of Lenhard and Parker (1990a). (For interpretation of the references to colour in this figure legend, the reader is referred to the web version of this article.)

Fig. 7. Predicted free (longer broken blue lines), residual (broken orange lines separated by two dots), entrapped (dotted grey line), and total (solid yellow line) LNAPL saturations as a function of elevation for the loamy sand for the same conditions as Fig. 6, but $S_{or}{}^{max}$ and $S_{oe}{}^{max}$ are 0.20 versus 0.15 (Fig. 6). The shorter broken black lines are estimates using the model of Lenhard and Parker (1990a). (For interpretation of the references to colour in this figure legend, the reader is referred to the web version of this article.)

LNAPL above z_u (i.e., $z_{ao} < z_{ao}{}^{max}$). To calculate $z_u{}^{max}$, we assume the same LNAPL well thickness as the current well thickness, i.e., we use $z_{ao}{}^{max}$ for z_{ao} in Eq. (22b) and $z_{ow}{}^{max}$ for z_{ow} where $z_{ow}{}^{max}$ = current $z_{ow} + z_{ao}{}^{max}$ – current z_{ao}. Using a different approach may artificially affect the total LNAPL volume in the subsurface media because the LNAPL thickness in the well will be different. Realistically, when fluid levels are raised creating entrapped LNAPL or lowered creating residual LNAPL above z_u, then less free LNAPL will be present and the LNAPL thickness in the well should change to reflect the volume of residual and entrapped LNAPL created.

For the 25 cm LNAPL thickness in the well (Fig. 4), the difference between the free LNAPL saturations and those predicted without considering residual and entrapped LNAPL (i.e., the short broken black lines) is not great. However, the predicted LNAPL transmissivity when accounting for residual and entrapped LNAPL above z_{ow} is 811.6 cm^2 day^{-1} [0.87 ft^2 day^{-1}]. The predicted LNAPL transmissivity when not accounting for residual and entrapped LNAPL is 1230 cm^2 day^{-1} [1.32 ft^2 day^{-1}], which is a 51.6% increase. The total LNAPL volume present when accounting for residual and entrapped LNAPL is 8.29 cm^3 cm^{-2}. When ignoring residual and entrapped LNAPL, the total LNAPL volume predicted is 4.30 cm^3 cm^{-2}.

Figs. 5 and 6 show the predicted free, residual, and entrapped LNAPL saturations for the loamy sand with the same 50 cm fluid level fluctuations as in Fig. 4. Fig. 5 shows the LNAPL distributions for a LNAPL well thickness of 50 cm with z_{ao} at 150 cm and z_{ow} at 100 cm. Fig. 6 shows the LNAPL distributions for a LNAPL well thickness of 100 cm with z_{ao} at 200 cm and z_{ow} at 100 cm. Development of the residual and entrapped LNAPL follow similar patterns as in Fig. 4, but the volumes of residual and entrapped LNAPL increase as LNAPL well thickness increases. In addition, the elevation over which LNAPL is present in the subsurface increases as LNAPL well thickness increases. In Fig. 4, LNAPL is present from an elevation of 75 cm to approximately 221 cm. In Fig. 6, LNAPL is present from an elevation of 50 cm to approximately 335 cm. The percentage of free LNAPL to total LNAPL also increases as LNAPL well thickness increases. The predicted LNAPL transmissivities when not accounting for residual and entrapped LNAPL are approximately 50% larger than the predicted LNAPL transmissivities when accounting for residual and entrapped LNAPL.

Fig. 7 shows the predicted free, residual, and entrapped LNAPL saturations for the loamy sand under the same conditions as Fig. 6, except $S_{or}{}^{max}$ and $S_{oe}{}^{max}$ are 0.20 versus 0.15. Because of the slight change, the predicted residual and entrapped LNAPL will be greater as will the predicted total LNAPL volume. For conditions in Fig. 7, the predicted total LNAPL volume is 33.78 cm^3 cm^{-2}, but for the

conditions in Fig. 6, it was 32.45 cm^3 cm^{-2}. The free LNAPL volume decreased from 24.04 to 22.55 cm^3 cm^{-2} for conditions in Fig. 6 versus Fig. 7. Consequently, the LNAPL transmissivity also decreased from 13,840 to 11,590 cm^2 day^{-1} [14.9 to 12.48 ft^2 day^{-1}] for the slight increase in the maximum residual and entrapped LNAPL saturations. The predicted LNAPL transmissivity, if residual and entrapped saturations are not accounted for (i.e., the short broken black lines), is 20,540 cm^2 day^{-1} [22.11 ft^2 day^{-1}], which is 77.2% higher than the predicted LNAPL transmissivity when accounting for residual and entrapped saturations. A slight change in $S_{or}{}^{max}$ and $S_{oe}{}^{max}$ can produce significant changes in the predicted LNAPL transmissivity.

To demonstrate potential consequences of not including or including effects of residual and entrapped LNAPL when managing LNAPL extraction from the subsurface, consider the loamy sand with a LNAPL well thickness of 18 cm: z_{ao} is at 150 cm and z_{ow} is at 132 cm. Further, consider the fluid levels in the well in the past fluctuated 50 cm (i.e., $z_{ao}{}^{max}$ is 200 cm and $z_{ow}{}^{min}$ is 82 cm). Lastly, assume estimates of $S_{or}{}^{max}$ and $S_{oe}{}^{max}$ equal to 0.15. The resulting predicted free, residual, and entrapped LNAPL saturations are shown in Fig. 8. Only entrapped LNAPL is present between elevations of 82 to 132 cm and the entrapped LNAPL saturation increases with elevation until the 132 cm elevation, current z_{ow}. Thereafter, the entrapped LNAPL saturations will decrease with elevation from 132 to 215 cm and approach zero at 215 cm; $z_u{}^{max}$
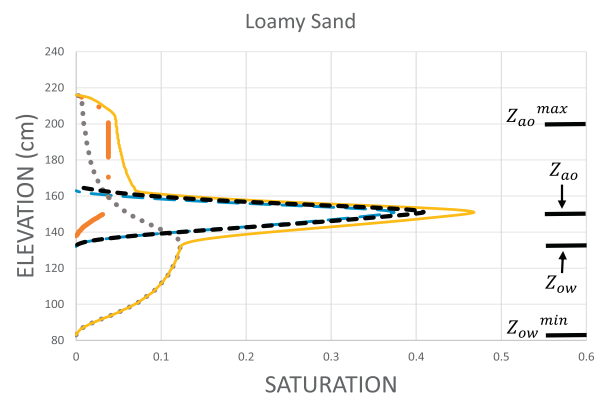
Fig. 8. Predicted free (longer broken blue lines), residual (broken orange lines separated by two dots), entrapped (dotted grey line), and total (solid yellow line) LNAPL saturations as a function of elevation for the loamy sand where $z_{ao} = 150$ cm, $z_{ow} = 132$ cm, $z_{ao}{}^{max} = 200$ cm, and $z_{ow}{}^{min} = 82$ cm elevations with $S_{or}{}^{max}$ and $S_{oe}{}^{max} = 0.15$. The shorter broken black lines are estimates using the model of Lenhard and Parker (1990a). (For interpretation of the references to colour in this figure legend, the reader is referred to the web version of this article.)

is approximately 215 cm. Residual LNAPL will begin to occur slightly above z_{ow}, 132 cm elevation, and increase to a maximum value. It will begin to decrease as the 215 cm elevation is approached because the conditions at which the largest residual LNAPL is created never develops. The free LNAPL occurs from approximately 132 to 165 cm; z_u is approximately 165 cm. The free LNAPL with positive fluid pressures (i.e., above atmospheric) is held from 132 to 150 cm elevation. The predicted LNAPL transmissivity for these conditions assuming the total liquid-saturated and vadose zones is 274.6 cm^2 day^{-1} [0.30 ft^2 day^{-1}]. Without accounting for residual and entrapped LNAPL, the predicted LNAPL transmissivity is 400.1 cm^2 day^{-1} [0.43 ft^2 day^{-1}].

Because LNAPL theoretically will only flow into a well under positive fluid pressures (above atmospheric), the LNAPL transmissivity that represents a recoverable rate can be predicted via Eq. (30) if the upper limit of integration is z_{ao} instead of z_u. We refer to this rate as the predicted LNAPL transmissivity of the total liquid-saturated zone, which for conditions in Fig. 8 is 88.8 cm^2 day^{-1} [0.10 ft^2 day^{-1}]. According to ITRC (2009), hydraulic or pneumatic LNAPL extraction systems may not be effective when LNAPL transmissivities are below 0.10 ft^2 day^{-1}. They further state some regulatory agencies have allowed LNAPL recovery (extraction) operations to close when there is demonstrated lack of recoverability (i.e., LNAPL transmissivity being low). For our hypothetical example, LNAPL extraction may be allowed to cease (technology end point) with a LNAPL well thickness of 18 cm if the effects of residual and entrapped LNAPL as well as the free LNAPL under positive pressures are accounted in LNAPL transmissivity estimations. If the effects of residual and entrapped LNAPL are not addressed, then predicted LNAPL transmissivities will be higher.

Over the total domain where LNAPL is predicted to exist in Fig. 8, the total LNAPL volume is 4.82 cm^3 cm^{-2}. The free, residual, and entrapped LNAPL volumes are 2.15, 1.02, and 2.86 cm^3 cm^{-2}, respectively. The free LNAPL volume in the total liquid-saturated zone is 1.23 cm^3 cm^{-2}. By applying the terms in the Model development section, predictions can be made that may help to design and operate subsurface LNAPL extraction technologies. In addition, technologies may be designed to target the entrapped and residual NAPL volumes such as groundwater drawdown or vacuum enhanced recovery. However, these need to be used with caution as they may lower the proportion of more easily recoverable LNAPL. It is likely that a sequential LNAPL recovery system will achieve the optimum results.

The effect of the magnitude of the fluid level fluctuations on predicted LNAPL transmissivity is shown by comparing Figs. 5 and 9 where the conditions for Fig. 9 are the same as Fig. 5, except the fluid level fluctuations are 75 cm versus 50 cm in Fig. 5. Both conditions assume

z_{ao} of 150 cm and z_{ow} of 100 cm. As can be seen, very similar patterns of free, residual, and entrapped LNAPL distributions result in both figures. The difference is the elevation range over which LNAPL is present in the loamy sand. For the 50 cm fluid level fluctuations (Fig. 5), LNAPL is predicted to exist from an elevation of 50 cm to approximately 242 cm. For the 75 cm fluid level fluctuations (Fig. 9), LNAPL is predicted to exist from an elevation of 25 cm to approximately 267 cm – a 50 cm difference. The greater are the fluctuations, then the 'smear' zone will become wider. The free LNAPL is predicted to exist over the elevation range from 100 cm to 168 cm regardless of the fluid level fluctuations. The free LNAPL is governed by the current fluid levels in the well and not prior levels. Consequently, the predicted LNAPL transmissivity over the liquid-saturated and vadose zones for the conditions in Fig. 9 is 4225 cm^2 day^{-1} [4.55 ft^2 day^{-1}], which is exactly the same as predicted for the conditions in Fig. 5. The predicted LNAPL transmissivity over only the liquid-saturated zone for the conditions in Fig. 9 is 3356 cm^2 day^{-1} [3.61 ft^2 day^{-1}], which is exactly the same as predicted for the conditions in Fig. 5.

The predicted LNAPL transmissivities for conditions in Figs. 5 and 9, however, are slightly lower than for conditions in *Scenario A* (Fig. 1), when there were no fluid level fluctuations. The reason is because larger amounts of residual LNAPL are predicted for conditions in Figs. 5 and 9 than for conditions in Fig. 1. $z_{ao}{}^{max}$ is greater than z_{ao} for conditions in Figs. 5 and 9, but $z_{ao}{}^{max}$ equals z_{ao} for the conditions in Fig. 1. The total residual LNAPL volumes predicted for conditions in Figs. 1, 5 and 9 are 1.78, 3.87, and 4.91 cm^3 cm^{-2}, respectively. Also, entrapped LNAPL is predicted for conditions in Figs. 5 and 9, but no entrapped LNAPL is predicted for conditions in Fig. 1. The total entrapped LNAPL volumes predicted for conditions in Figs. 1, 5 and 9 are 0, 2.95, and 4.47 cm^3 cm^{-2}, respectively. Hence, there are higher free LNAPL saturations over the total liquid-saturated and vadose zones for conditions in Fig. 1 than in Figs. 5 and 7, which results in a slightly higher LNAPL transmissivity prediction over the total liquid-saturated and vadose zones for conditions in Fig. 1. The total free LNAPL volumes predicted for conditions in Figs. 1, 5 and 9 are 10.25, 9.91, and 9.91 cm^3 cm^{-2}, respectively; however, the free LNAPL volume over only the total liquid-saturated zone are identical for conditions in Figs. 1, 5, and 9. The predicted LNAPL transmissivity over the total liquid-saturated and vadose zones for conditions in Fig. 1 is 4294 cm^2 day^{-1} [4.62 ft^2 day^{-1}] and the predicted LNAPL transmissivity over the total liquid-saturated zone is 3356 cm^2 day^{-1} [4.62 ft^2 day^{-1}]. The predicted LNAPL transmissivities over only the total liquid-saturated zone for conditions in Figs. 5 and 9 are the same as for conditions in Fig. 1. The important element is LNAPL transmissivities are largely a function of current fluid levels in wells and not historic levels. Accounting for fluid level fluctuations in the subsurface will provide information concerning the range of elevations where subsurface LNAPL may be present. Further, the predicted actual total volume of LNAPL in the subsurface will be larger if residual and entrapped LNAPL are considered. This may impact the management of LNAPL remedial actions of sites.

5. Summary & conclusions

An approach is developed to predict free, residual, and entrapped LNAPL saturations as a function of static fluid levels measured in wells. The approach also accounts for historic effects of fluctuating fluid levels. Integrating the saturations over a vertical slice of the subsurface yields the LNAPL specific volumes. After accounting for residual and entrapped LNAPL volumes, the LNAPL transmissivities over the total liquid-saturated and vadose zones are predicted. LNAPL transmissivity and the free LNAPL specific volume over the total liquid-saturated zone are estimates of the rate of LNAPL flow through a vertical slice of the subsurface toward a well and the recoverable LNAPL from pumping extraction technologies.

LNAPL specific volumes and transmissivities are predicted for two hypothetical porous media: a loamy sand and a clay loam. Predictions
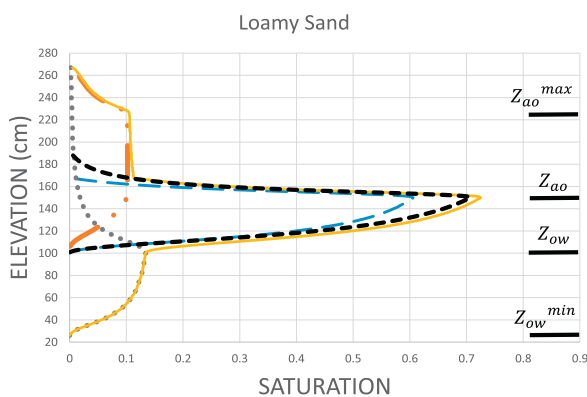
Fig. 9. Predicted free (longer broken blue lines), residual (broken orange lines separated by two dots), entrapped (dotted grey line), and total (solid yellow line) LNAPL saturations as a function of elevation for the loamy sand where $z_{ao} = 150$ cm, $z_{ow} = 100$ cm, $z_{ao}{}^{max} = 225$ cm, and $z_{ow}{}^{min} = 25$ cm elevations with $S_{or}{}^{max}$ and $S_{oe}{}^{max} = 0.15$. The shorter broken black lines are estimates using the model of Lenhard and Parker (1990a). (For interpretation of the references to colour in this figure legend, the reader is referred to the web version of this article.)

are developed for different LNAPL thicknesses in a well and for different ranges of fluid level fluctuations to demonstrate results from the model. One key result is the elevation range from the LNAPL-water interface in a well to the upper elevation where the free LNAPL saturation approaches zero is the same regardless of porous media type for a given LNAPL thickness in a well. Any difference in the free LNAPL thickness in porous media will be related to the thickness of a well-defined, water-saturated capillary fringe for porous media types. The LNAPL specific volume, however, corresponding to the LNAPL thickness in a well is dependent on porous media type. Another key result is the free LNAPL transmissivities, whether over the total liquid-saturated and vadose zones or only over the total liquid-saturated zone, are largely a function of the current fluid levels in a well and not historic levels. Therefore, it may not be necessary to know fluid level fluctuations if LNAPL transmissivity of the total liquid-saturated zone may be the primary prediction of concern. Lastly, a slight change in S_{or}^{max} and S_{oe}^{max} can produce significant changes in the predicted LNAPL transmissivity.

The predictions using the approach estimate the form of the LNAPL (i.e., free, residual, and entrapped) at elevations in the subsurface. The approach is unique in that elevation-dependent (non-constant) residual and entrapped LNAPL saturations are predicted and accounted for in LNAPL transmissivity estimates. The elevation-dependent LNAPL saturations are useful for assessing potential groundwater contamination risks and possible regions where different technologies may need to be employed other than LNAPL extraction from wells to lower potential groundwater contamination risks. With knowledge of historic fluid level fluctuations, the region where only residual LNAPL exists in the vadose zone can be identified in which vapor extraction technologies can be employed to lower contamination risks. The predictions, especially the LNAPL transmissivity over the total liquid-saturated zone, may indicate when LNAPL subsurface extraction via pumping may be at a technology end point. The approach can be valuable to practitioners conducting subsurface LNAPL remediation as well as regulators who oversee LNAPL remediation. The accuracy of the predictions are dependent on attainment of static fluid levels in wells (i.e., near vertical equilibrium conditions) and proper assignment of porous medium and fluid parameters.

Acknowledgements

References

Aral, M.M., Liao, B., 2002. Effect of groundwater table fluctuations on LNAPL thickness in monitoring wells. Environ. Geol. 42, 151–161.

Ballestero, T.P., Fiedler, F.R., Kinner, N.E., 1994. An investigation of the relationship between actual and apparent gasoline thickness in a uniform sand aquifer. Ground Water 32, 708–718.

Brooks, R.H., Corey, A.T., 1966. Properties of porous media affecting flow. J. Irrig. And drain. Div. ASCE. 92, 61–88.

Carsel, R.F., Parrish, R.S., 1988. Developing joint probability distributions of soil water retention characteristics. Water Resour. Res. 24, 755–769.

Charbeneau, R.J., 2007. LNAPL distribution and recovery model (LDRM). In: Volume 1: Distribution and Recovery of Petroleum Hydrocarbon Liquids in Porous Media. API Publ. No. 4760. American Petroleum Institute, Washington, D.C..

Charbeneau, R.J., Johns, R.T., Lake, R.W., McAdams, M.J., 2000. Free-product recovery of petroleum hydrocarbon liquids. Ground Water Monitoring & Remediation 20, 147–158.

van Dam, J., 1967. The migration of hydrocarbons in a water-bearing stratum. In: The Joint Problems of the Oil and Water Industries: Proceedings of a Symposium Held at the Hotel metropole, Brighton. 18–20. Institute of Petroleum, London, pp. 55–96 January 1967.

Davis, G.B., Johnston, C.D., Thierrin, J., Power, T.R., Patterson, B.M., 1993. Characterising the distribution of dissolved and residual NAPL petroleum hydrocarbons in unconfined aquifers to effect remediation. AGSO. J. Aust. Geology Geophysics 14, 243–248.

Farr, A.M., Houghtalen, R.J., McWhorter, D.B., 1990. Volume estimation of light nonaqueous phase liquids in porous media. Ground Water 28, 48–56.

van Genuchten, M.Th., 1980. A closed-form equation for predicting the hydraulic conductivity of unsaturated soils. Soil Sci. Soc. Am. J. 44, 892–898.

Hall, R.A., Blake, S.B., Champlin Jr., S.C., 1984. Determination of hydrocarbon thickness in sediments using borehole data. In: Proceeding of the 4th National Symposium on Aquifer Restoration and Ground Water Monitoring. National Water Well Assoc, pp. 300–304.

Hampton, D.R., Miller, P.D.G., 1988. Laboratory investigation of the relationship between actual and apparent product thickness in sands. In: Conf. Petroleum Hydrocarbons and Organic Chemicals in Ground Water: Prevention, Detection and Restoration, National Water Well Assoc, pp. 157–181.

ITRC (Interstate Technology & Regulatory Council), 2009. Evaluating LNAPL remedial technologies for achieving project goals. In: LNAPL-2. Interstate Technology & Regulatory Council, Washington D.C. (157 pp.).

Jeong, J., Charbeneau, R.J., 2014. An analytical model for predicting LNAPL distribution and recovery from multi-layered soils. J. Contam. Hydrol. 156, 52–61.

Johnston, C.D., 2010. Selecting and assessing strategies for remediating LNAPL in soils and aquifers. In: CRC CARE Technical Report No. 18. CRC for Contamination Assessment and Remediation of the Environment, Adelaide, Australia (178 pp).

Johnston, C.D., Adamski, M., 2005. Relationship between initial and residual LNAPL saturation for different soil types. In: Proceedings of the 2005 Petroleum Hydrocarbons and Organic Chemicals in Groundwater®: Prevention, Assessment, and Remediation Conference. 17-19 August, Costa Mesa, pp. 29–42.

Johnston, C.D., Trefry, M.G., 2009. Characteristics of light nonaqueous phase liquid recovery in the presence of fine-scale soil layering. Water Resour. Res. 45, W05412. http://dx.doi.org/10.1029/2008WR007218.

Johnston, C.D., Rayner, J.L., Briegel, D., 2002. Effectiveness of in situ air sparging for removing NAPL gasoline from a sandy aquifer near Perth, Western Australia. J. Contam. Hydrol. 59, 87–111.

Kaluarachchi, J.J., Parker, J.C., 1992. Multiphase flow with a simplified model for oil entrapment. Transp. Porous Media 7, 1–14.

Lenhard, R.J., Parker, J.C., 1987. Measurement and prediction of saturation-pressure relationships in three phase-porous media systems. J. Contam. Hydrol. 1, 407–424.

Lenhard, R.J., Parker, J.C., 1988. Experimental validation of the theory for extending two phase saturation-pressure relations to three fluid phase systems for monotonic drainage paths. Water Resour. Res. 24, 373–380.

Lenhard, R.J., Parker, J.C., 1990a. Estimation of free hydrocarbon volume form fluid levels in monitoring wells. Ground Water 28, 57–67.

Lenhard, R.J., Parker, J.C., 1990b. Discussion of estimation of free hydrocarbon volume form fluid levels in monitoring wells. Ground Water 28, 800–801.

Lenhard, R.J., Oostrom, M., Dane, J.H., 2004. A constitutive model for air-NAPL-water flow in the vadose zone accounting for immobile, non-occluded (residual) NAPL in strongly water-wet porous media. J. Contam. Hydrol. 73, 283–304.

Marinelli, F., Durnford, D.S., 1996. LNAPL thickness in monitoring wells considering hysteresis and entrapment. Ground Water 34, 405–414.

Matos de Souza, M., Oostrom, M., White, M.D., da Silva Jr, G.C., Barbosa, M.C., 2016. Simulation of subsurface multiphase contaminant extraction using a bioslurping well model. Transp. Porous Media 114, 649–673.

Mercer, J.W., Cohen, R.M., 1990. A review of immiscible fluids in the subsurface: properties, models, characterization and remediation. J. Contam. Hydrol. 6, 107–163.

Newell, C.J., Acree, S.D., Ross, R.R., Huling, S.G., 1995. Light nonaqueous phase liquids. In: U.S.EPA, R.S. Kerr Environ. Res. Lab. Ada OK. EPA/540/S-95/500, (28 pp.).

Parker, J.C., Lenhard, R.J., 1987. A model for hysteretic constitutive relations governing multiphase flow, 1. Saturation-pressure relations. Water Resour. Res. 23, 2187–2196.

Parker, J.C., Lenhard, R.J., 1989. Vertical integration of three phase flow equations for analysis of light hydrocarbon plume movement. Transp. Porous Media 3, 187–206.

Parker, J.C., Lenhard, R.J., Kuppusamy, T., 1987. A parametric model for constitutive properties governing multiphase flow in porous media. Water Resour. Res. 23, 618–624.

Parker, J.C., Kaluarachchi, J.J., Kremesec, V.J., Hockman, E.L., 1990. Modeling free product recovery at hydrocarbon spill sites. In: Conf. Petroleum Hydrocarbons and Organic Chemicals in Ground Water: Prevention, Detection and Restoration, National Water Well Assoc. pp. 641–655.

Parker, J.C., Zhu, J.L., Johnson, T.G., Kremesec, V.J., Hockman, E.L., 1994. Modeling free product migration and recovery at hydrocarbon spill sites. Ground Water 32, 119–128.

de Pastrovich, T.L., Baradat, Y., Barthel, R., Chiarelli, A., Fussell, D.R., 1979. Protection of groundwater from oil pollution. In: CONCAWE Report 3/79. The Hague, Netherlands (61 pp.).

Rayner, J.L., Johnston, C.D., Rao, P.S.C., 2000. Characterising residual NAPL using partitioning and interfacial tracers and implications for interphase mass transfer. In: Johnston, C.D. (Ed.), Contaminated Site Remediation: From Source Zones to Ecosystems. Proc. 2000 Contaminated Site Remediation Conference, Melbourne, Victoria, 4-8 December, 2000pp. 613–620.

Rayner, J.L., Snape, I., Walworth, J.L., Harvey, P.McA., Ferguson, S.H., 2007. Petroleum–hydrocarbon contamination and remediation by microventing at subAntarctic Macquarie Island. Cold Reg. Sci. Technol. 48, 139–153.

Schwille, F., 1967. Petroleum contamination of the subsoil: a hydrological problem. In: Brighton (Ed.), The Joint Problems of the Oil and Water Industries: Proceedings of a Symposium Held at the Hotel Metropole, Brighton, 18–20 January 1967. Institute of Petroleum, London, pp. 23–54.

Sookhak Lari, K., Davis, G.B., Johnston, C.D., 2016a. Incorporating hysteresis in a multiphase multi-component NAPL modelling framework; a multi-component LNAPL gasoline example. Adv. Water Resour. 96, 190–201.

Sookhak Lari, K., Johnston, C.D., Davis, G.B., 2016b. Gasoline multi-phase and multi-

component partitioning in the vadose zone: dynamics and risk longevity. Vadose Zone J. 15 (3). http://dx.doi.org/10.2136/vzj2015.07.0098.

Steffy, D.A., Johnston, C.D., Barry, D.A., 1995. A field study of the vertical immiscible displacement of LNAPL associated with a fluctuating water table. In: Groundwater Quality: Remediation and Protection. IAHS Publ. No. 225, pp. 49–57.

Steffy, D.A., Barry, D.A., Johnston, C.D., 1997a. Improved scaling technique for two phase pressure saturation relationships. J. Contam. Hydrol. 28, 207–225.

Steffy, D.A., Barry, D.A., Johnston, C.D., 1997b. Influence of antecedent moisture content on residual LNAPL saturation. J. Soil Contam. 6, 113–147.

Steffy, D.A., Johnston, C.D., Barry, D.A., 1998. Numerical simulations and long-column tests of LNAPL displacement and trapping by a fluctuating water table. J. Soil Contamination 7, 325–356.

Suthersan, S., Koons, B., Schnobrich, M., 2015. Contemporary management of sites with petroleum LNAPL presence. Ground Water Monitoring & Remediation 35 (1), 23–29.

Van Geel, P.J., Roy, S.D., 2002. A proposed model to include a residual NAPL saturation in a hysteretic capillary pressure-saturation relationship. J. Contam. Hydrol. 58, 79–110.

Waddill, D.W., Parker, J.C., 1997. Simulated recovery of light, nonaqeoous phase liquid from unconfined heterogeneous aquifers. Ground Water 35, 938–947.

White, M.D., Oostrom, M., Lenhard, R.J., 2004. A practical model for mobile, residual and entrapped NAPL in water-wet porous media. Ground Water 42, 734–746.

Wipfler, E.L., van der Zee, S.E.A.T.M., 2001. A set of constitutive relationships accounting for residual NAPL in the unsaturated zone. J. Contam. Hydrol. 50, 53–77.

Zilliox, L., Muntzer, P., 1975. Effects of hydrodynamic processes on the development of ground-water pollution: Study on physical models in a saturated porous medium. Progress in Water Tech. 7, 561–568.